Journal of Applied Mathematics and Computational Mechanics 2025, 24(2), 18-32
www.amcm.pcz.pl p-ISSN 2299-9965
DOI: 10.17512/jamcm.2025.2.02 e-ISSN 2353-0588

STUDY OF THE STRESS-STRAIN STATE OF A PERFORATED PLATE WITH STIFFENING RIBS

Michał Bembenek[1], Saltanat Nurkusheva[2], Vasyl Mykhailiuk[3], Ryszard Machnik[1]

[1] *Faculty of Mechanical Engineering and Robotics, AGH University of Krakow Krakow, Poland*
[2] *Department of Transport Equipment and Technology, S. Seifullin Kazakh Agrotechnical Research University, Astana, Kazakhstan*
[3] *Ivano-Frankivsk National Technical University of Oil and Gas Ivano-Frankivsk, Ukraine*
bembenek@agh.edu.pl, saltanat.nurkusheva@kazatu.kz, myhajlyukv@ukr.net, machnik@agh.edu.pl

Received: 17 October 2024; Accepted: 8 May 2025

Abstract. This study investigates the mechanical behaviour of solid and perforated plates with stiffening ribs through a systematic three-stage approach integrating simulation and experimental methods. Initial investigations focused on the formation of stiffeners, revealing that rupture ceased at a hole diameter of 10 mm, with maximum equivalent stresses reaching 275 MPa. Using ANSYS Workbench, we analysed the stress-strain state and stability characteristics, finding a critical load of 43 N for stability loss in the perforated plates. Experimental results indicated that a perforated plate deflected 10.35 mm under a load of 38.5 N, whereas a solid plate exhibited the same deflection under only 11.5 N, indicating a 70 % difference in load capacity. Additionally, the weight of the solid plate was measured at 92.8 grams, compared to 76.6 grams for the perforated plate, achieving a weight reduction of over 17 %. These findings highlight the superior structural performance and material efficiency of perforated plates with stiffening ribs. The study underscores the potential for optimizing engineering designs to enhance functionality and reduce material usage.

MSC 2010: *7405, 74G70*
Keywords: *perforated plates, stress, displacement, deformation, mass, stiffening ribs, ANSYS simulation*

1. Introduction

Perforated steel sheets are often used in a variety of machines and equipment. Perforated plates with stiffeners are widely used in various branches of engineering due to their ability to increase the stability of structures. They are most common in the aviation and automotive industries, shipbuilding, construction, mechanical engineering (in the structures of mechanisms, support systems in various machines: housings, bottoms, discs, filters, etc.). The presence of holes in steel sheets definitely affects their mechanical properties [1]. It should be noted that the use of perforated sheets when they are subjected to perpendicularly directed loads requires the use of special edges (stiffeners). The strength and stability of the perforated steel sheet will depend on the shapes and geometric parameters of these ribs [2].

When a load is applied to a perforated sheet, there exists a limit beyond which its stability may be lost; such an effect encompasses a sudden deformation that is achieved as the stored membrane (axial) energy is converted to bending energy while the external loads are kept constant. It is not difficult to analyze the loss of stability of a perforated plate using SolidWorks Simulation software through linearized techniques that include approximating the critical coefficients of stability loss and the corresponding modes of instability [3].

A perforated sheet can take various configurations during deformation for various load magnitudes [4]. The form that the sheet assumes when losing stability is referred to as the mode of loss of stability, under conditions of "critical" loading. Analysis of stability loss simplifies the determination of the various "mod" modes. In practice, researchers and designers take into consideration the first fundamental mode (mode 1) since it is the one that corresponds to the lowest value of load. Where loss of stability is a major design factor, determination of the different modes of stability loss helps to indicate weaknesses in the model. The mode characteristics of the loss can guide the adaptation of the model or supporting system, reducing the potential for buckling at the respective modes [5].

2. Literature review

In recent years, there has been a large increase in interest in the investigation of perforated stiffened plates due to their favorable mechanical characteristics in relation to solid plates [1]. A survey of the literature indicates an extensive body of research on the stress-strain behavior [6], stability [7], and optimization of these structures [8-11].

Initial studies of perforated plates were concerned mainly with their applications in different branches of engineering. Researchers have reported benefits of saving mass of the material without sacrificing the structural strength, which has helped open doors for more complicated studies on their mechanical behavior.

A significant body of research employs finite element analysis (FEA) methodologies, specifically the ANSYS Workbench, for simulating the behavior of perforated plates subjected to different loading conditions [12-14]. Recent research underscores the success of these simulations at predicting the stress-strain response as well as the likely failure locations. Comparison with other modeling methodologies demonstrates that FEA offers a better representation of complicated geometries and loading conditions [15].

Introduction of stiffening ribs significantly affects the mechanical behavior of perforated plates. It is already established by previous research that these ribs enhance the load-carrying capacity while, simultaneously, minimizing deflection.

Further analysis considering fracture development during the plastic deformation of stiffeners has been developed, discussing the necessity of knowing their behavior under adverse environments [16]. Research shows that optimization of the position of the ribs can result in overall improved performance.

One of the most significant areas of the existing literature investigates the conditions of stress and strain in perforated and solid plates [6]. Various techniques have been suggested to quantify loss of stability, with a specific focus on perforated structures. Comparisons reveal that perforated plates have greater buckling resistance [17, 18], thereby widening their use in structural design [7].

Physical experiments are required in laboratory tests for the validation of simulation results. Many researchers have concentrated on performing physical experiments for checking the deflection and load-carrying ability of perforated and solid plates. The results always validate the theoretical predictions, affirming the enhanced performance of perforated designs [1].

The research reported in [8] involved an investigation on the pre-critical and first post-critical equilibria of longitudinally compressed reinforced plates by considering multiple critical loads.

The reinforced plates were simulated with flat four-node elements, and the analysis involved geometric nonlinearity with the assumption of elastic material fully. The research formulated techniques of investigating the stability of these plates, calculating the critical forces of different thicknesses. Further, the study designed graphs illustrating the deflection versus compressive loads relationship, investigating the influence of initial geometric imperfections on the critical force values of the reinforced plates. Perforated steel plate shear walls (PSPSWs) are known for their wide applications in different pieces of equipment, as referenced in [9]. It is observed through research that PSPSWs increase plasticity, leading to an exploration of topology optimization to design a new PSPSW. The study experimented with four values of aspect ratio (0.67, 1.0, 1.5, and 2.0) and three plate thicknesses (2 mm, 4 mm, and 8 mm). The result of the topological optimization was compared with three conventional round-hole PSPSW designs and a previously optimized design, while keeping the material volume constant between plates with the same aspect ratios and thicknesses. Cyclic behavior of all the models was compared to enable comparison of strength, energy absorption, and failure modes. The analytical hierarchy process was used to evaluate and find out the best model and configuration that was effective, and the results showed that the optimized designs showed increased performance. The results indicated that the optimized model achieved a score of 22.07 %, which was higher than the scores of the previous optimized model and three traditional models, which had scores of 20.67 %, 19.36 %, 19.06 %, and 18.84 %, respectively. Topology optimization was also employed in [10] to determine the geometric characteristics, size, and distribution of voids in a novel perforated steel plate shear wall (PSPSW). The model relied on a new design called the annular steel plate shear wall. Strain energy was employed as the objective function for the optimization. Four initial slab configurations relative to the length of the column-to-slab connection were proposed in the study. Eight cases and seven perforated plates through topological optimization were given, with nonlinear analyses for both cyclic and monotonic loading conditions. Cyclic and monotonic response, pinching effects, stiffness characteristics, load-carrying capacity, energy dissipation mechanisms, fracture behaviors, and out-of-plane deformations were the key concerns. The results demonstrated that the optimized models exhibited improved performance compared to the annular model, but all with the identical initial volume of the plates. Research on perforated steel sheets has highlighted the necessity to study their behavior under the action of uniaxial tensile loading [11]. The presence of holes greatly influences the mechanical properties of these steel sheets. This work focused on investigating the stress-strain relation of perforated steel sheets using the finite element method as an analysis tool. Experimental tests were conducted on developed prototypes to validate the results of the simulations. The result indicated that the finite element method was effective in the precise computation of the stress-strain behavior of perforated steel sheets. Importantly, it was found that the influence of diamond-shaped perforations was higher compared to other shapes, whereas square perforation did not have any effect on the engineering stress-strain relationship. Furthermore, the efficiency of linear or staggered perforated shapes regarding the effective net area exposed to applied loads was found to decrease load-carrying capacity [19, 20] for both types of perforation.

In spite of the loss, the configurations improved the overall properties of the steel sheets. The literature corroborates the demand for ongoing research in this area, specifically new material development and novel manufacturing processes. Research in the future may target the environmental impacts of perforated plate application and exploration of novel designs with significantly improved performance.

In summary, there is a solid base of research that explains the behavior of stiffened perforated plates. The combination of simulation and experimental methods has been successful in developing an understanding of the subject, and this has resulted in encouraging applications in contemporary engineering.

The purpose of the work is to study solid and perforated plates with stiffeners to compare their mechanical characteristics. To achieve the set goal, it is necessary to:

- prepare experimental full-scale samples of a flat and perforated plate with holes;
- create three-dimensional models of a flat and perforated plate with holes for further simulation modeling;
- determine the mechanical characteristics of full-scale samples of the studied plates on a special stand and the mechanical characteristics of sample models using simulation modeling;
- compare the results obtained and draw appropriate conclusions.

3. Experimental

3.1. Research methods

The investigation of solid and perforated plates reinforced with stiffening ribs is conducted in a systematic three-stage approach:

1. Formation of Stiffeners. The initial phase involves examining the formation of stiffeners on perforated plates. This stage aims to assess the potential for breakage in the stiffeners during plastic deformation, thereby evaluating their structural integrity under stress.
2. Stress-Strain State and Stability Analysis. The second phase focuses on analyzing the stress-strain state of both solid and perforated plates with stiffening ribs. This includes a study of the stability loss in perforated plates, facilitating a comparative analysis of the mechanical behavior of solid versus perforated configurations.
3. Laboratory Validation. The final stage encompasses laboratory experiments on manufactured perforated plates equipped with stiffening ribs. This phase serves to validate the findings from simulation modeling and laboratory research, particularly through a comparison of deflections observed in both solid and perforated plates.

This multi-faceted approach ensures a thorough understanding of the mechanical properties and performance of the studied plates, contributing to the optimization of their design in engineering applications.

The stress-strain state of perforated plates was analyzed using the finite element method. Further derivations were developed on the basis [21] and were not derived by the authors of the article. In applying the principle of minimum potential energy for approximate solutions through finite element analysis, the domain is divided into multiple subregions called «elements», denoted as *N*. The total potential energy of the system equals the sum of potential from all subregions:

$$\pi = \sum_{i=1}^{N} \pi_i, \text{ where: } \pi = \int_{V_i} \left[\varepsilon^T C \left(\frac{1}{2}\varepsilon - \overline{A}\Delta T \right) - f^T u \right] dV - \int_{S_{\sigma_i}} t^T u dS \tag{1}$$

here, V_i represents the volume of the i^{th} element, and S_{σ_i} denotes the boundary portion subject to surface traction.

Within each element, the displacement matrix u is expressed as:

$$u_i = D_i \cdot q_i \tag{2}$$

where q_i contain nodal displacements and their derivatives, while D_i consists of interpolation functions that define displacement variations within the element. To ensure continuity across the domain, adjoining elements must share identical displacements and functional representations at common nodal boundaries. The strain matrix ε_i is derived as:

$$\varepsilon_i = B_i \cdot q_i \tag{3}$$

where B_i contains position-dependent function. This leads to

$$\pi_i = q_i^T \left(\frac{1}{2} k_i \cdot q_i - F_i \right), \text{ where: } k_i = \int_{V_i} B_i^T C_i \, B_i \; dV$$

and

$$F_i = \int_{V_i} D_i^T f \, dV + \int_{S_{\sigma_i}} D_i^T t_n \, dS + \int_{V_i} B_i^T \, C_i \, \overline{A_1} \, \Delta T_i \, dV \quad (4)$$

Here, k_i denotes the element stiffness matrix, whose components represent equivalent nodal forces consistent with the assumed displacement distribution.
Through mathematical manipulation, the system's total potential energy:

$$\pi = \sum_{i=1}^{B} \pi_i, \text{ where: } \pi = q^T \left(\frac{1}{2} Kq - F \right) \quad (5)$$

where q contains all nodal displacement, K is the assembled global stiffness matrix, and F is the global nodal load matrix. These are related by:

$$q_i = M_i \cdot q \quad (6)$$

with M_i mapping local displacement q_i to the global matrix q. Then the stiffness matrix K is given by

$$K = \sum_{i=1}^{N} M_i^T \, k_i \, M \quad (7)$$

and

$$F = \sum_{i=1}^{N} M_i^T \, F_i \quad (8)$$

The system's potential energy requires optimization relative to all unconstrained nodal parameters (displacement and their derivatives, totaling M variables). Concurrently, boundary nodes on surface must adhere to specified displacement requirements. This dual condition establishes

$$\delta\pi = \sum_{j=1}^{M} \frac{\partial \pi}{\partial q_j} \delta q_i = 0 \quad (9)$$

where the summation encompasses all unspecified parameters q_j. Since the values of δq_j are arbitrary, the minimization procedure leads to the set of equations

$$\frac{\partial \pi}{\partial q_j} = 0 \quad j = 1, 2, \ldots M \quad (10)$$

The system contains precisely q_j independent equations matching the unknown variables. The resulting numerical solution provides approximate nodal quantities that converge toward exact values as discretization refines. These computed parameters subsequently enable stress field reconstruction through the constitutive relationship

$$\sigma_i = C_i B_i q_i \tag{11}$$

3.2. Study of the formation of stiffeners on a perforated plate

In preparation for the subsequent stages of the research, a detailed investigation of the formation of stiffeners on a perforated plate was conducted. The plate had a thickness of 0.5 mm, and a series of holes with varying diameters (ranging from 7.5 mm to 10 mm in increments of 0.5 mm) were introduced. The application of a ball with a diameter of 12.5 mm to these holes resulted in the rupture of the formed stiffening ribs. Notably, the rupture of the stiffener was observed to cease when the diameter of the drilled hole reached 10 mm.

Figure 1 illustrates the stiffeners formed at different diameters of drilled holes in the perforated plate, providing visual representation of the structural changes induced by the hole sizes.

Fig. 1. Formed stiffeners for different diameters of drilled holes in a perforated plate

It should also be noted that the formation of stiffeners on the tested plate with holes required a special mandrel (guiding mandrel), since without its use the formed stiffeners were irregular in shape.

The investigated plate is made of steel grade 08 ps. Its mechanical characteristics are: Young's modulus $2 \cdot 10^{11}$ Pa, Poisson's ratio 0.28, yield strength 196 MPa, tensile strength 360 MPa.

3.3. Simulation modelling

To analyze the stress-strain state and evaluate the loss of stability in the perforated plate with stiffeners, the ANSYS Workbench software was employed. This software uses the finite element method. For the second stage of the research, a three-dimensional model was constructed for both solid and perforated plates with stiffening ribs, as depicted in Figure 2. The overall dimensions of the plates were consistent, measuring 110 mm by 215 mm with a thickness of 0.5 mm.

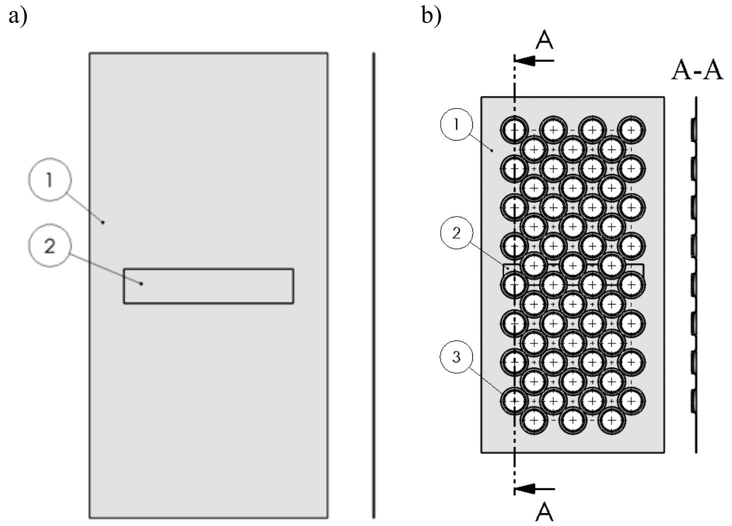

Fig. 2. Three-dimensional models of plates: a) solid, b) perforated with stiffening ribs;
1 – plate, 2 – platform for applying the load, 3 – holes with stiffening ribs

To perform the second stage of research (determining the stress-strain state of solid and perforated plates, studying the loss of stability of the perforated plate), the calculation scheme shown in Figure 3 was developed.

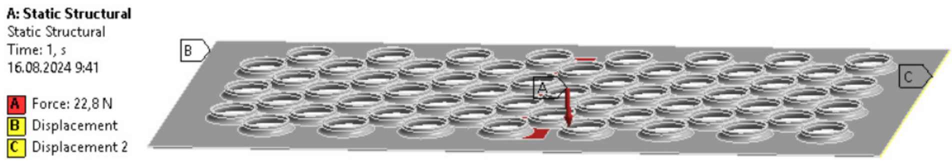

Fig. 3. Calculation scheme

According to this scheme (Fig. 3), a given load (A) is applied to a given platform, ensuring the identity of the geometric dimensions and the location of the platforms for both the solid and perforated plates. To maintain consistency of the boundary conditions that will be used during simulation modeling and laboratory experiments, constraints were applied to the ends of the plates (B, C) to prevent downward motion. Motion in all other directions was allowed.

The Newton-Raphson numerical method was used during simulation modeling.

The properties of the material for simulation modeling of the plate are taken to correspond to the properties of the material from which the solid and perforated sheets for full-scale studies are made (steel grade 08 ps): Young's modulus $2 \cdot 10^{11}$ Pa, Poisson's ratio 0.28, yield strength 196 MPa, tensile strength 360 MPa. The finite element mesh utilized in the analysis is shown in Figure 4.

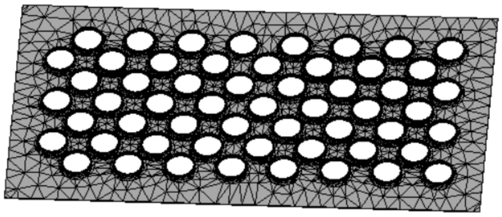

Fig. 4. Mesh of finite elements

A linear analysis approach was adopted, considering the linear behavior of the material throughout the study.

3.4. Laboratory studies

For conducting laboratory studies, models of plates were made: solid and perforated with stiffening ribs (Fig. 5).

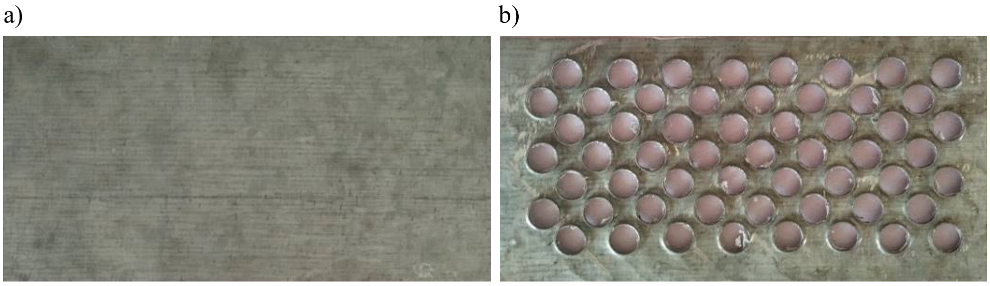

Fig. 5. Manufactured plates for laboratory research: a) continuous, b) perforated with stiffening ribs

The production of the perforated plate was carried out by pre-drilling the holes and then pressing them with a hardened steel ball with a diameter of 12.5 mm. Perforated and solid plates are made of cold-rolled carbon steel (grade 08 ps).

3.5. Stand for laboratory research

A special stand (Fig. 6) has been developed for conducting laboratory studies of manufactured plates (solid and with perforated holes with stiffening ribs). The stand consists of the following main parts: supports 1 and 4, on which the tested plate 3 is installed. The load on plate 3 is transmitted from axis 2, which is connected to the dynamometer 7. To control the deflection of the plate (in the middle of the plate – maximum movements), a displacement indicator is used 6, which is installed on the holder 5. A holder (not shown in Fig. 6) is attached to the dynamometer 6, on which the loads are installed.

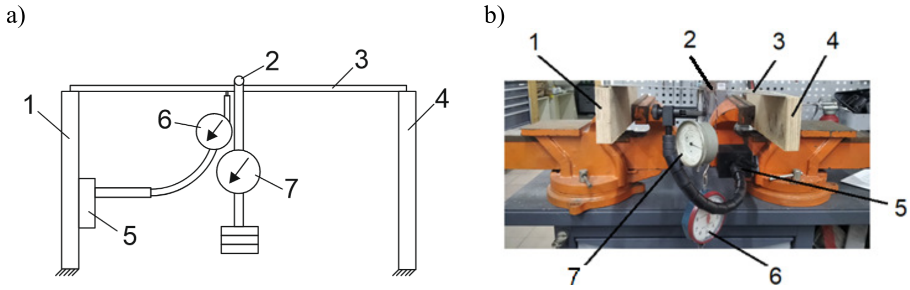

Fig. 6. Stand for plate research: a) diagram, b) construction; 1, 4 – support, 2 – axis, 3 – the investigated plate, 5 – holder of the displacement indicator, 6 – movement indicator, 7 – dynamometer

4. Results

Results of the second stage of the study (study of the stress-strain state of solid and perforated plates, study of the loss of stability of the perforated plate, comparison of the results of the study of solid and perforated plates).

So, Figure 7 shows a deflection of 8.4 mm under a load of 30 N.

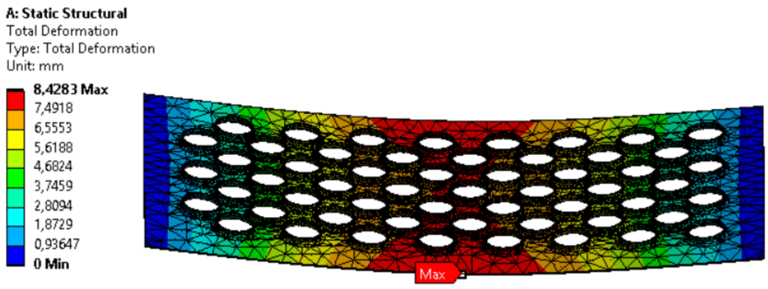

Fig. 7. Deflection of the plate

In order to verify the operation of the boundary conditions, Figure 8 shows the movement along the Y-axis of the edge of the plate.

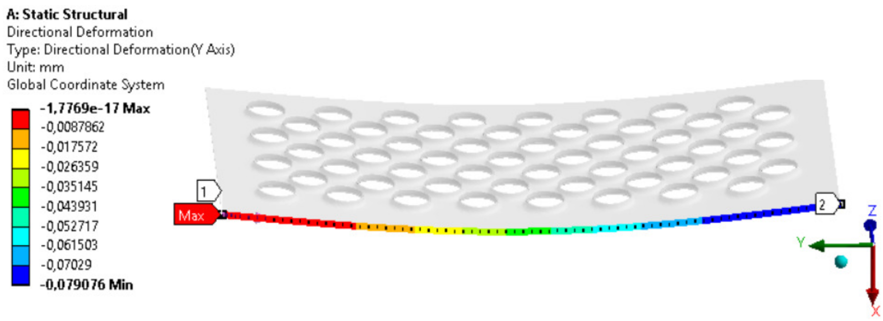

Fig. 8. Moving along the Y axis of the edge of the plate

Figure 9 shows the distribution of equivalent stresses in the plate under the action of a force of 30 N.

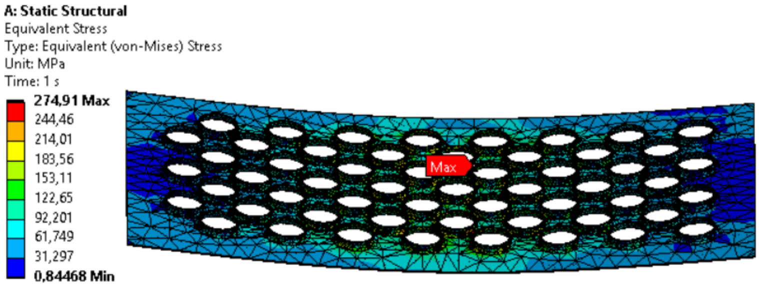

Fig. 9. Distribution of equivalent stresses

Therefore, the maximum equivalent stresses occurring in a perforated plate with stiffeners are 275 MPa and are observed at the end of the stiffener. No plastic deformation is observed when the plate is loaded with 30 N.

Figure 10 shows the movement in a solid plate under a load of 6.2 N.

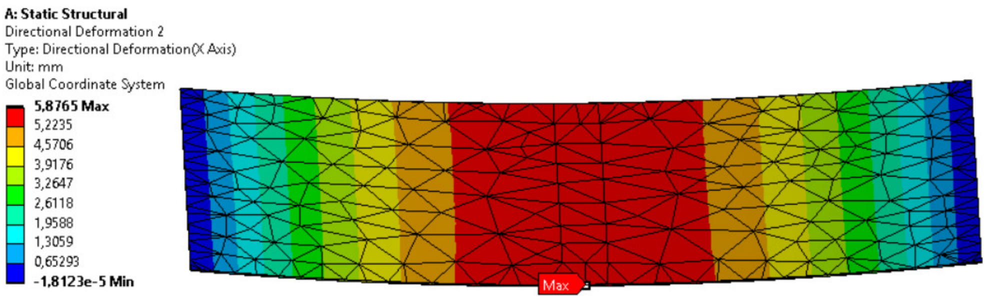

Fig. 10. Deformation in a solid plate under a load of 6.2 N

Figure 11 shows the dependence of the amount of deflection of solid and perforated plates with stiffening ribs on the applied load.

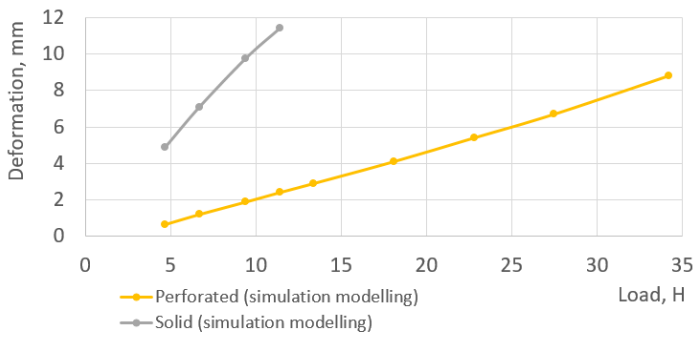

Fig. 11. Dependence of the amount of deflection of solid and perforated plates with stiffening ribs on the applied load

Regarding the study of the loss of stability of perforated plates with stiffeners, the Eigenvalue Buckling module of the Ansys Workbench program was used to determine the amount of load that would lead to a loss of stability. This value is equal to 43 N.

Figure 12 shows the results of the study of the loss of stability of a perforated plate with stiffening ribs.

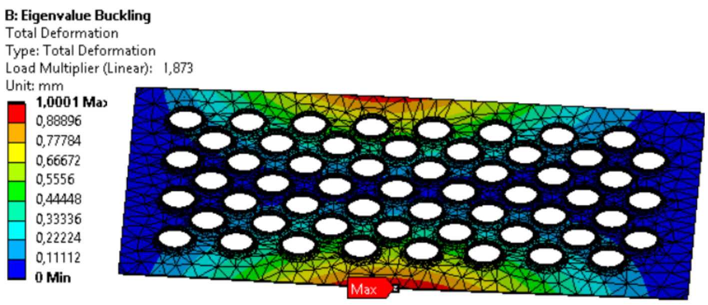

Fig. 12. The results of the study of the loss of stability of a perforated plate with stiffening ribs

The results of the third stage of research (laboratory) of solid and perforated plates with stiffening ribs are shown in Figure 13. This figure shows graphical dependences of plate deflection depending on the applied load.

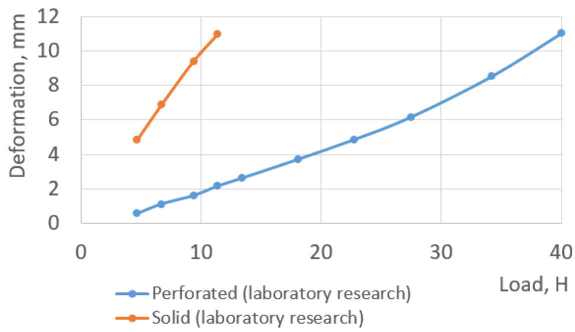

Fig. 13. Dependence of plate deflection on the applied load

According to Figure 13, a deflection of 10.35 mm occurs in a solid plate under a load of 11.5 N. In contrast, a perforated plate with stiffeners deflects by the same amount under a load of 38.5 N (70 % difference).

At the same time, the mass of a solid plate is 92.8 grams, and the mass of a perforated plate with stiffening ribs is 76.6 grams (a difference of more than 17 %).

To verify the results of simulation modelling and laboratory research (comparison of the deflection of solid and perforated platinum), the graphic dependencies shown in Figure 14 were constructed.

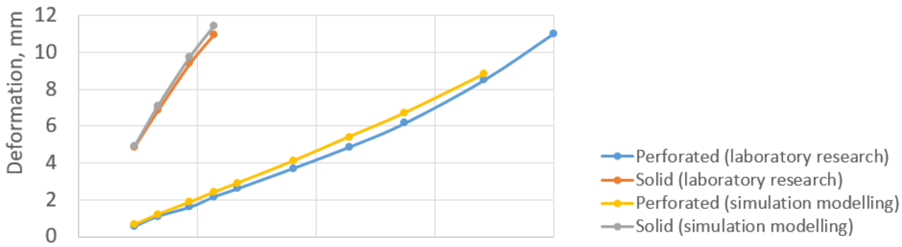

Fig. 14. Dependence of plate deflection on the applied load

Analysing the results of the studies shown in Figure 14, there is a slight discrepancy between the results obtained using the finite element method and laboratory studies.

5. Conclusions

This study provides an analysis of the mechanical behaviour of solid and perforated plates with stiffening ribs, employing a multi-stage approach that integrates both simulation and experimental methodologies. The results demonstrate that perforated plates exhibit significant advantages in terms of deflection and weight efficiency compared to their solid counterparts. Specifically, the findings indicate that a perforated plate with stiffeners deflects 10.35 mm under a load of 38.5 N, while a solid plate exhibits a deflection of 10.35 mm under only 11.5 N, highlighting a 70 % difference in load capacity.

The investigation into the formation of stiffeners revealed critical insights regarding the rupture behaviour under loading conditions, with the maximum equivalent stress in the perforated plate reaching 275 MPa at the end of the stiffener. This study found that the rupture of the stiffener ceased at a hole diameter of 10 mm, indicating the importance of hole dimensions in maintaining structural integrity.

The Eigenvalue Buckling analysis indicated that the critical load leading to stability loss in the perforated plates was determined to be 43 N. Laboratory validation confirmed the simulation results.

The significant difference in weight between the solid and perforated plates – 92.8 grams for the solid plate versus 76.6 grams for the perforated plate – underscores the potential for material optimization in engineering applications, achieving a weight reduction of over 17 %.

Acknowledgements

The results presented in the article will be a part of S. Nurkusheva PhD thesis.

References

[1] Luo, Z., Zhao, H., Qiao, D., Zhang, Y., An, J., Tan, C., Liang, L., Liu, A., & Shao, X. (2024). Shear behavior on PBL shear connector with a relatively thin perforated steel plate in steel-UHPC composite bridge deck system. *Engineering Structures*, *316*, 118583.

[2] Rahmonov, B.S., Karimov, I.M., Narzulloyev, M.A., Sobirova, R.A., & Almuratov, S.N. (2024). Action of moving load on a ribbed cylindrical shell with viscoelastic filler. API Conference Proceedings, *3045*(1), 030099.

[3] https://help.solidworks.com/2023/russian/SolidWorks/cworks/c_Linearized_Buckling_Analysis.htm?id=78b31d81063348a8a778699ff348adff#Pg0.

[4] Ren, C., Liu, Q., Wang, B., & Dai, L. (2020). Numerical analysis and design method of cold-formed thin-walled c-section steel perforated member. *Journal of Shanghai Jiaotong University, 54*(10), 1084-1093.

[5] Rozylo, P. (2024). Limit states of thin-walled composite structures with closed sections under axial compression. *Composites Part B: Engineering*, *287*, 111813.

[6] Romaniuk, V., Bezniuk, L., Supruniuk, V., Kononchuk, O., Meshcheryakova, O., & Sorochak, A. (2024). Features of the work of continuous perforated beams near intermediate supports. *Procedia Structural Integrity*, *59*, 471-478.

[7] Huang, X., Zhou, Z., Shen, Y., Zhao, J., & Li, R. (2024). Post-fire mechanical properties and constitutive modeling of LY225 low-yield strength steel. *Journal of Constructional Steel Research*, *221*, 108923.

[8] Manuylov, G.A., Kositsyn, S.B., & Grudtsyna, I.E. (2020). Numerical analysis of stability of the stiffened plates subjected aliquant critical loads. *Structural Mechanics of Engineering Constructions and Buildings*, *16*(1), 54-61.

[9] Bagherinejad, M.H., & Haghollahi, A. (2020). Study on topology optimization of perforated steel plate shear walls in moment frame based on strain energy. *International Journal of Steel Structures*, *20*, 1420-1438.

[10] Bagherinejad, M.H., & Haghollahi, A. (2019). Topology optimization of perforated steel plate shear walls with thick plate in simple frames. *Iran University of Science & Technology*, *9*(3), 457-482.

[11] Sayed, A.M. (2019). Numerical analysis of the perforated steel sheets under uni-axial tensile force. *Metals*, *9*(6), 632.

[12] Patil, R.A., & Salgar, P.B. (2024). Experimental investigation on structural behaviour of castellated column under axial load. *Asian Journal of Civil Engineering*, *25*(6), 4645-4655.

[13] Bartus, J., & Odrobinak, J. (2024). On the shear force redistribution in composite steel and concrete beams with web openings. *Buildings*, *14*(6), 1658.

[14] De'nan, F., Wai, C.S., & Hashim, N.S. (2024). Impact of web perforation size and shapes on structural behavior: a finite element analysis. *World Journal of Engineering*, *21*(5), 911-923.

[15] Derda, T. (2022). Suddenly loaded arrays of pillars with variable range of load transfer. *Journal of Applied Mathematics and Computational Mechanics*, *21*(4), 16-27.

[16] Sun, L., Liu, Y., Wang, H., Shi, F., Liu, J., & Jiang, L. (2023). Tensile stiffness of perfobond rib connectors in steel-concrete composite pylon of bridges. *Engineering Structures*, *284*, 115931.

[17] Neiva, L., Braz Starlino, J.A., Elias, G., Cunha Sarmanho, A.M., & Nicchio Alves, V. (2022). Industrial storage system continuous perforated uprights: a combined design proposal. *Revista de la Construcción*, *21*(2), 204-214.

[18] Deng, X., Chen, Zh., & Zhou, Yu. (2010). Effects of gaps and bearing types on performance of perforated triple-steel tube buck ling-restrained brace. *Journal of Earthquake Engineering and Engineering Vibration*, *30*(3), 64-69.

[19] Xu, X., Liu, Y., & Zuo, Y. (2018). Contribution of perforated steel ribs to load-carrying capacities of steel and concrete composite slabs under negative bending. *Advances in Structural Engineering*, *21*(12), 1879-1894.

[20] Erdal, F. (2016). Effect of stiffeners on failure analyses of optimally designed perforated steel beams. *Steel and Composite Structures*, *22*(1), 183-201.

[21] *Theoretical Manual SolidWorks Simulation*. (2015). Dassault Systèmes.